Mechanical Properties of Pyrolytic Graphite

J. J. GEBHARDT* AND J. M. BERRY†
General Electric Company, Philadelphia, Pa.

A series of mechanical strength and thermal expansion tests has been carried out from room temperature to 5000°F on the two microstructural types of current production pyrolytic graphite. Results indicate that with appropriate precautions in selecting test material, machining, and testing specimens, current production pyrolytic graphites yield higher, more reliable mechanical property values. The contribution of process improvements to this increase cannot be specifically separated although it may show up principally in allowing more of a given batch of material to be selected. The present series of tests show that both types of pyrolytic graphite tested have similar ultimate *a* direction tensile strengths in the vicinity of 18,000 ±2100 psi at room temperature, rather than previously found values of 11,000 ± 5000 psi. The largest difference between surface nucleated and continuously nucleated material was observed in torsional tests parallel to the planes; values of 1555 ± 60 and 2880 ± 245 psi, respectively, were obtained throughout the temperature range to 5000°F. This difference is also due to microstructural effects. Significant differences between the flexure strengths of the two materials were observed which can be attributed to microstructure. Little effect of microstructure was seen in reversible thermal expansion measurements although larger irreversible changes occurred in continuously nucleated specimens.

I. Introduction

ALTHOUGH pyrolytic graphite has become widely known[1–6] as a material of unusual properties and great promise in aerospace technology, little appears to have been published recently regarding its mechanical properties. Aside from the data obtained during the early phases of its commercial development, much of the test data appear only in individual, rather restricted test programs, and are not widely circulated.[7, 8]

Inasmuch as considerable refinement of the manufacturing process has occurred since the early test data were gathered, there is some question as to how realistically these early data represent the properties of pyrolytic graphite as it is currently manufactured. Current manufacturing techniques yield two general microstructural variations that are distinctive in appearance and which may be suspected to have different mechanical properties.

The purpose of this program was two-fold: to determine the mechanical properties of currently produced materials of both structural types, and to establish the degree to which differences between the properties of the two materials may be attributed to their characteristic structures.

II. Pyrolytic Graphite

It is important to consider, in the beginning, the features of pyrolytic graphite which make it unusual and which make testing it somewhat more difficult than conventional materials.

Pyrolytic graphite is a polycrystalline form of graphite deposited from the vapor phase at high temperatures (circa 4000°F) by thermal decomposition of a simple hydrocarbon such as methane. The deposits consist of layers of wavy and kinked planes of hexagonally arranged carbon atoms, mutually parallel but randomly rotated about an axis perpendicular to the plane of the deposit. In customary terminology, this axis is known as the *c* axis or direction whereas the direction parallel to the planes is referred to as the *a-b* direction. The microstructures of the deposits vary with processing conditions and have intimate influence on the properties of the deposits.[3] In general, two representative classes of structures have become known. These are the so-called surface nucleated and continuously nucleated or regenerative pyrolytic graphite. Figure 1 illustrates the gross differences between them. Figure 1a shows the former type in which the growth or cone structure originates at the first deposited layer and is propagated in uninterrupted fashion to the top of the deposit. The regenerative structure however is continuously interrupted by additional nuclei or growth origins laid down throughout manufacture and presents the aspect shown in Figure 1b. It should be emphasized that all variations between these extremes can and are produced with associated effects on the material properties. Thus, pyrolytic graphite is essentially a class of materials, the specific properties of each member being dependent on its characteristic microstructure.

The layered structure, with strong covalent bonding in the planes and weak electrostatic (van der Waals) bonding between the planes, leads to a high degree of anisotropy in all properties.[4] Depending on processing conditions, the degree of crystallite order in the *a-b* direction may vary. These differences may be measured and spoken of as variations in degree of preferred orientation or in the degree to which a given array of nearly parallel crystallites deviates from being perfectly parallel to each other and to the *a-b* plane.

Pyrolytic graphite is inherently brittle at room temperature and therefore subject to serious damage and premature failure if the surfaces of test specimens are not carefully finished. Thus, the scatter band in a given series of test results can be expected to be somewhat broader than would be the case for ductile materials. In addition to anisotropy and brittleness, random process variations from batch to batch can also induce, among other things, isolated nodules that serve as stress raisers, high grain boundary angles, and delaminations. All of these serve to lower test values and to increase their scatter.

Proper selection of material, careful attention to machining and alignment, and examination of fracture surfaces can serve, however, to reduce the scatter, to explain unexpectedly

Received April 20, 1964; revision received September 25, 1964. The authors gratefully acknowledge the support of the Special Projects Office, Naval Bureau of Weapons, in carrying out the program through which the results presented in this paper were obtained. The authors are also greatly indebted to R. F. Berning and his associates of the General Electric Company Research Laboratory, Schenectady, New York, for their care, skill, and continued interest in performing all of the mechanical and thermal tests reported here.

* Physical Chemist, Missile and Space Division.
† Physical Metallurgist, Missile and Space Division.

low values, and generally, to increase the working knowledge of pyrolytic graphite, which is necessary to achieve the full potential of its mechanical properties.

With these considerations in mind, a test program was developed to obtain reliable data on specimens characteristic of current production of the two general structural types described previously. It was not considered in any sense a statistical evaluation, but was aimed instead at explaining a broad scatter band and the relatively low values of room temperature measurements made earlier.[7]

Previous experience[8] showed the necessity for selecting material not obviously defective, whereas other work[9] pointed out the need for careful machining and alignment of test specimens. Consequently, considerable attention was paid to details in these areas.

III. Experimental Results and Discussion

The following measurements were carried out on both continuously nucleated and surface nucleated pyrolytic graphite as functions of temperature up to 5000°F: 1) ultimate tensile strength in the *a* direction, 2) torsional strength in the *a* direction, 3) flexure strength both parallel and perpendicular to the *c* axis by three and four point loading, 4) elastic modulus in the *a* direction, and 5) linear thermal expansion in the *a* and *c* directions.

Material representative of current production was received as deposited, from the Metallurgical Products Department, General Electric Company [surface nucleated (SN)] and the Raytheon Manufacturing Co., [regenerative or continuously nucleated (CN)]. Densities were 2.20 and 2.206 g/cm, respectively, measured by immersion in alcohol. Depositions were made at 4000°F and no subsequent heat treatment or annealing was done. Microstructures of the two types of material are shown in Figs. 1a and 1b. These are typical of both materials, the entire lot in each case having come from a single production run.

Test specimens were cut from flat plate raw stock and all surfaces were finished by grinding with a relatively soft wheel (SiC, 100 grit, H-bond, vitrified) rotating at 5000 surface ft/min.

Measurements at elevated temperatures were made under helium in a graphite resistance heated furnace. Temperatures were approached as rapidly as possible followed by a 5 min soak at test temperature. In tests at 5000°F, the specimen was also heated as rapidly as possible, but the soak time was adjusted to include the period required to go from 4000° to 5000°F. Thus all specimens tested at 5000°F were above the deposition temperature (4000°F) for about the same length of time.

A. Ultimate Tensile Strength

Ultimate tensile strength parallel to the planes was measured at room temperature and up to 5000°F using an Instron testing machine. Viewing ports and telescopes permitted visual observation and measurement during testing. Tests at room temperature were run in laboratory atmosphere with transverse and longitudinal strain gages (Budd Company #C61X1-M50A) attached using Eastman 910 cement. The tensile specimen was 2 in. wide at the gripping ends and narrowed to a gage section of 0.200 in. × 0.200 in. Over-all length was 6 in. and effective gage length was 1.5465 in. Cross head motion was 0.020 in./min. The procedure and specimen design were slightly modified for tests at 5000°F by reducing the gage cross section to 0.200 in. deep by 0.125 in. wide and increasing the cross head speed to 0.050 in./min. This was done to insure gage length failure and to compensate for the elongation of the specimen.

The results of the tensile tests are shown in Fig. 2 and Table 1. The values listed are all gage length failures except for the two so designated at 5000°F. Earlier values[7] are also shown at the 50 and 90% confidence levels for comparison.

B. Torsional Strength

Torsional strength is defined as the resistance of the specimen to shearing forces generated by rotation about the *c* axis when torque is applied to the specimen in a direction parallel to the planes. Specimens were designed, loaded, and fractured in torsional testing up to 5000°F in the manner shown in Fig. 3. The octagonal faces of the specimens fitted into similary shaped wells in the ends of rotating graphite rods. No clamping force was applied to the specimen faces

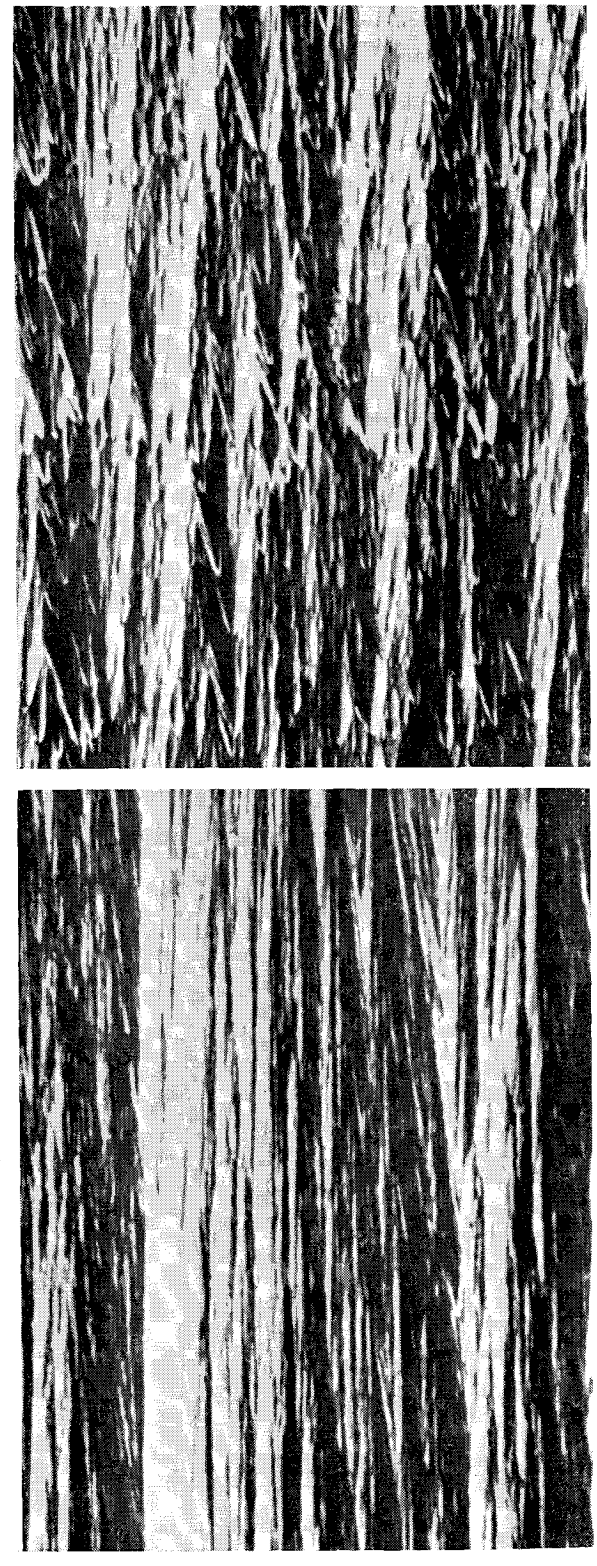

Fig. 1 Microstructure of surface nucleated and continuously nucleated pyrolytic graphite.

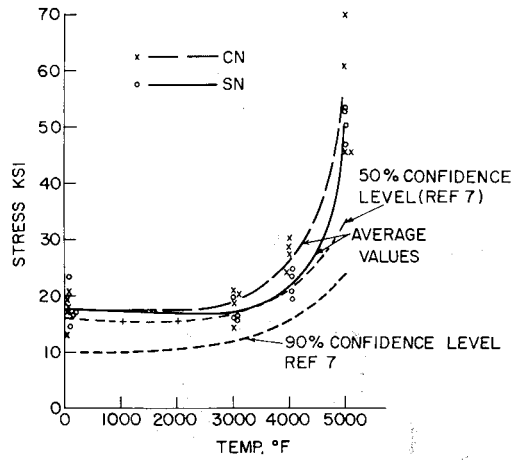

Fig. 2 Tensile strength of pyrolytic graphite vs temperature, °F.

in the direction of c axis while the rods, and hence the opposing faces of the specimen, were being rotated in opposite directions around the c axis as indicated in Fig. 3. Cross head motion and thermal cycle were the same as for tensile tests. The results are listed in Fig. 4 and Table 2.

The higher values characteristic of the continuously nucleated material reflect the increased "interlocking" caused by the continued formation of new growth cones during deposition. Such interlocking is characteristic of a somewhat lower degree of preferred orientation in the material and is responsible for the differences in mechanical, electrical, and thermal properties of surface nucleated and continuously nucleated pyrolytic graphite.

C. Flexure Strength

Flexure tests were carried out at temperatures up to 5000°F using both three and four point loading techniques with the last deposited surface of the material in tension. Tests were made with loading applied both parallel and perpendicular to the c axis. Beams were $2\frac{1}{4}$ in. long and 0.200 in. square, all sides ground flat and parallel. In the 3-point loading tests, the span was $1\frac{1}{2}$ in., whereas in 4-point loading, the loading bars were 2 in. apart on the tensile side and 1 in. apart on the compressive side. Longitudinal and transverse strain gages were attached to several of the room temperature, 4-point load tests to obtain tensile and compressive modulus data. Results are summarized in Tables 3 and 4 and Figs. 5 and 6.

Differences between the two test materials are most pronounced with loading in the direction parallel to the c axis.

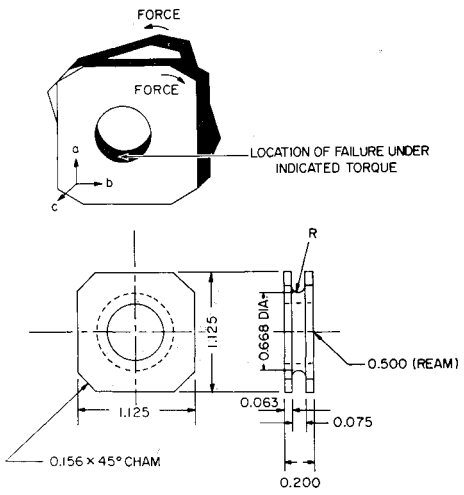

Fig. 3 Torsion test specimen.

Table 1 Tensile strength of pyrolytic graphite vs temperature, °F

Temperature, °F		CN, psi	SN, psi
75		17,864	17,462
		19,219	17,409
		18,296	23,677
		20,557	14,630
		13,156	17,107
	avg	17,818 ± 1865	18,191 ± 2328
3000		18,700	15,900
		20,600	15,800
		14,150	19,800
		20,500	16,175
	avg	18,488 ± 2169	16,919 ± 1441
4000		24,200	19,580
		28,600	24,800
		30,000	23,400
		27,300	20,600
	avg	27,525 ± 1775	22,095 ± 2005
5000		>45,600	50,000
		60,500	53,400
		45,100	>52,100
		69,900	46,600
	avg	>55,275 ± 9925	>50,525 ± 2225
		> = Pin failure	

Failure in the surface nucleated material occurred chiefly by delamination near the neutral axis, the region of maximum shear stress. On the other hand, continuously nucleated specimens failed by basal plane tension almost exclusively.

In general, the use of flexure test results as an index of tensile strength does not appear to be definitive. Factors such as resolved stresses, beam thickness, microstructure, method of loading, and mode of failure all serve to confuse interpretation of results with respect to probable tensile strengths at failure. However, from a practical point of view, since flexural loading is common to many useful configura-

Table 2 Torsional strength of pyrolytic graphite vs temperature, °F

Temperature, °F		CN, psi	SN, psi
75		2333	1887
		2522	1032
		2309	1790
		2339	1484
		2887	1416
	avg	2578 ± 205	1522 ± 253
3000		2953	1476
		2182	1761
		2143	1555
		3109	447[a]
		2874	1631
	avg	2652 ± 392	1374 ± 331
			1606 ± 90[b]
4000		3070	1348
		3240	891
		3094	1740
			1570
			1795
	avg	3135 ± 70	1469 ± 280
5000		2848	915
		3214	2028
		3397	1097
		3070	1968
		3248	2090
	avg	3155 ± 157	1620 ± 491

[a] Did not fail in gage section.
[b] Average excluding low value.

Table 3 Flexure test results; continuously nucleated pyrolytic graphite

Temperature, °F		3 Perpendicular, ksi	3 Parallel, ksi	4 Perpendicular, ksi	4 Parallel, ksi
75		25.7	20.8	26.2	20.0
		23.4	21.8	19.9	19.1
		24.6	20.8	26.3	19.6
		23.8	22.8	23.7	22.1
		24.8	19.4	21.6	13.3
		23.6	22.6	24.4	22.3
		23.8	19.4	21.7	16.9
		25.1	21.0	21.2	20.5
		20.2	22.0	24.0	18.6
		23.8	9.7	20.6	18.7
	avg	23.9	20.0	23.0	19.1
3000		27.3	21.6	25.5	24.6
		28.0	23.8	25.3	20.3
		28.1	25.3	26.9	21.9
	avg	27.8	23.5	25.9	22.3
4000		31.0	32.3	28.7	28.4
		29.0	30.9	31.3	24.4
		33.0	33.5	33.1	31.8
	avg	31.0	32.2	31.0	28.2
5000		23.8NF	19.0NF	26.6NF	29.7NF

tions, flexure test data must be obtained and interpreted with all of the preceding factors in mind.

D. Elastic Modulus

Elastic moduli shown in Fig. 7 were computed for both surface and continuously nucleated material from the strain gage data obtained at room temperature in both tension and 4-point bend tests, as well as from direct observation at elevated temperatures. Here again, a significant difference is seen as a result of microstructural variation. The surface nucleated material is somewhat stiffer throughout the temperature range than is the continuously nucleated material.

Table 4 Flexure test results; surface nucleated pyrolytic graphite

Temperature, °K		3 Perpendicular, ksi	3 Parallel, ksi	4 Perpendicular, ksi	4 Parallel, ksi
75		21.6	12.7	21.3	11.2
		21.4	11.5	12.7	9.4
		20.7	20.0	18.0	10.0
		22.6	17.2	18.8	14.7
		13.4	16.1	13.7	14.3
		22.3	16.3	16.2	12.4
		17.6	18.5	20.4	6.8
		21.5	15.1	16.4	14.1
		23.9	13.5	17.2	16.4
		20.7	19.2	19.0	12.1
	avg	20.6	16.0	17.5	12.1
3000		20.0	14.9	20.9	14.9
		20.6	17.3	21.8	11.3
		23.0	19.9	16.3	10.9
	avg	21.2	17.4	19.7	12.4
4000		23.9	19.0	15.1	14.9
		24.2	22.2	18.6	16.7
		22.4	20.4	15.4	12.4
	avg	23.5	20.5	16.4	14.7
5000		29.1	46.4NF	23.0	18.3

On an absolute scale, however, the difference is not large, both materials being characterized as having relatively low moduli, although they are from 2 to 3 times higher than a good grade of hot pressed graphite.[10] Strain gage measurements on the 4-point bend specimens were used to calculate room temperature moduli for both tensile and compressive surfaces. These values are listed in Table 5 along with Poisson's ratios determined from dimensional changes occurring during room temperature tensile tests. The negative sign associated with these ratios is probably the result of flattening out of the "wrinkles"

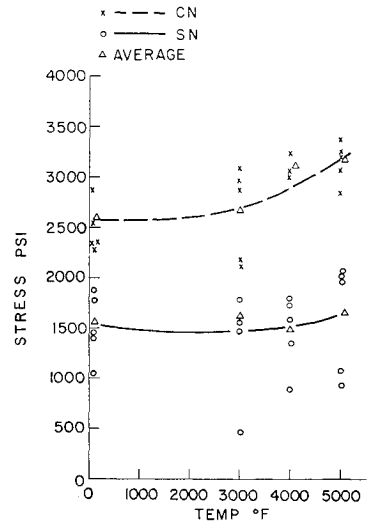

Fig. 4 Torsional strength of pyrolytic graphite vs temperature.

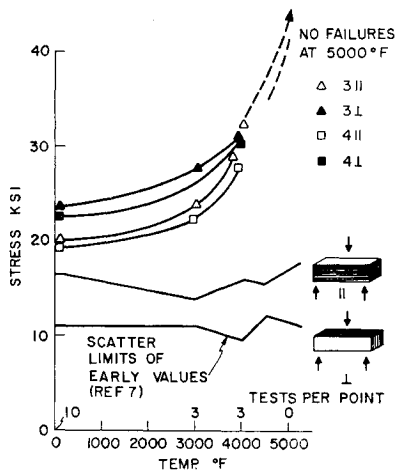

Fig. 5 Average flexure strength of pyrolytic graphite (continuously nucleated) vs temperature, °F. 3- and 4-point loading.

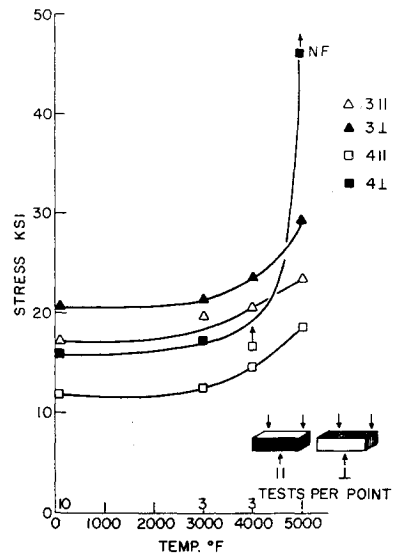

Fig. 6 Average flexure strength of pyrolytic graphite (surface nucleated) vs temperature, °F. 3- and 4-point loading.

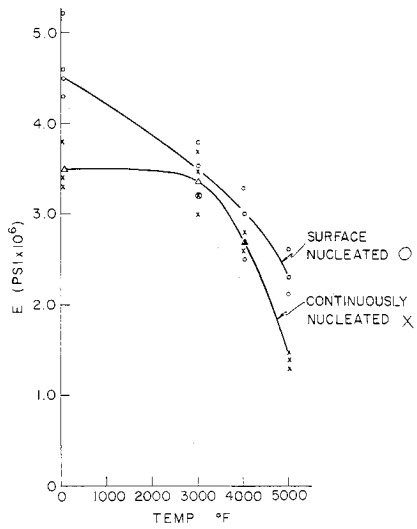

Fig. 7 Elastic modulus pyrolytic graphite *a* direction vs temperature.

characteristic of the basal planes of pyrolytic graphite, the net result being an increase in the *a* and *b* direction dimensions and a decrease in the *c* or interplanar dimension.

E. Thermal Expansion

Results of thermal expansion measurements, made in the *a* and *c* directions for the two test materials are shown in Figs. 8 and 9, respectively. As can be seen from the descending portion of the curve in Fig. 8, there appears to be a permanent elongation in the *a*-*b* direction for both grades of material, which is somewhat greater for the continuously nucleated material than for surface nucleated material. This is due to the annealing and flattening out of "wrinkles" and kinks in the basal planes which are somewhat more pronounced for the highly nucleated structure. The effect of this on the *c* direction expansion is to cause a partial reversal or decrease in thickness at elevated temperatures as the specimen is permitted to remain at test temperature. This is indicated by the downward turn at the end of the *c* direction expansion curve (Fig. 9). The calculated coefficients of expansion over the linear portions of the curves do not indicate very much effect of microstructure on the apparent thermal anisotropy

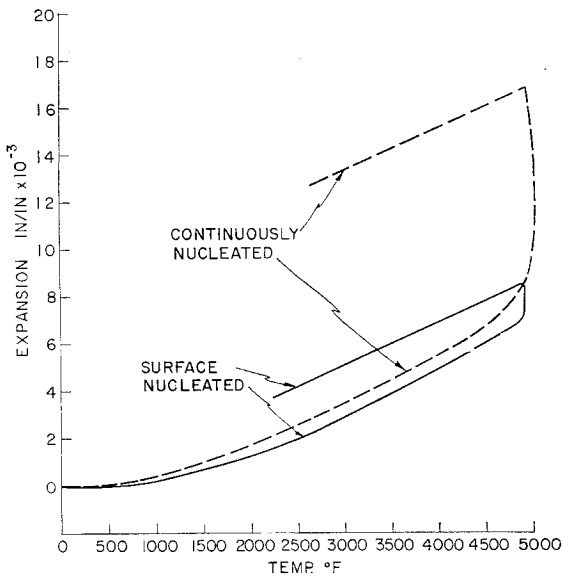

Fig. 8 Thermal expansion pyrolytic graphite *a* direction vs temperature.

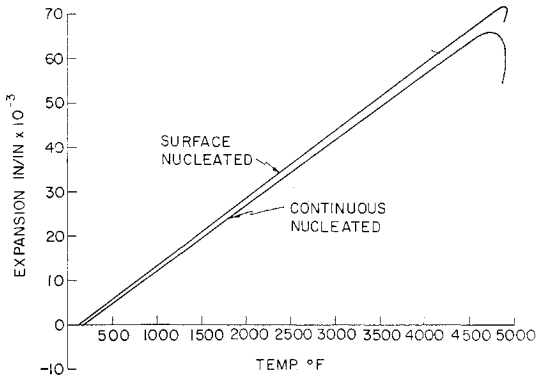

Fig. 9 Thermal expansion pyrolytic graphite *c* direction vs temperature, °F.

ratios for the two materials. Certainly, variation in microstructure is a much less obvious factor here than in the case of torsional and flexure tests.

IV. Surface Preparation Microstructure and Test Results

As is commonly observed in the case of brittle materials, machining and surface finishing procedures have a profound effect on test results. This is illustrated by the fact that tensile specimens, which failed at low stress values in room temperature tests, did so by basal plane failure at grips, an occurrence also noted in earlier test reports. Examination of such specimens after flame polishing[11] to bring out structural features, showed considerable delamination emanating from the edge of the grip hole (Fig. 10). In effect, these specimens had been severely notched prior to test. Remachining of untested specimens and retesting of broken specimens using fillet grips gave higher tensile strength values with failures occurring in the gage length. Further examination of certain tensile specimens after fracture revealed characteristic fracture surfaces, indicating that, although failure had occurred in the gage length, the mode of failure was by basal plane failure initiating at one edge of the gage section, propagating horizontally across the gage section. In effect, this amounts to a flexure test with loading perpendicular to the *c* axis. This could have been easily brought about by slight misalignment or by relatively minor machine damage to the plane edges in the gage section.

Examination of the edges of flexure test beams also brought out the fact that structural differences in pyrolytic graphite can produce various responses to the same grinding technique. Beams made from continuously nucleated material showed little or no visible damage, whereas the surface nucleated beams nearly always had notches and chip-outs at the corners and edges. Thus the lower degree of interplanar interlocking characteristic of surface nucleated material is also

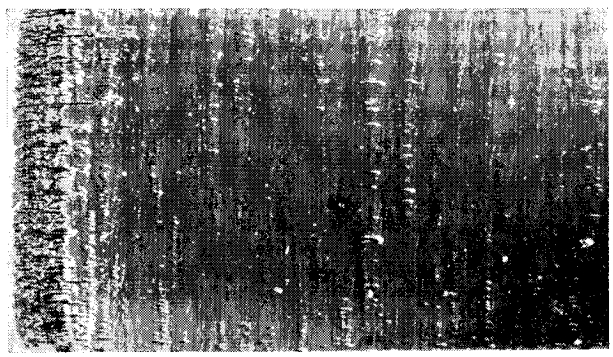

Fig. 10 Damaged region around grip-hole in tensile specimens (flame polished).

Table 5 Poisson's ratios and elastic modulus 75°F (strain gage determination on 4-point bend tests)

Stress, ksi	Material	Top surface	Substrate side	*c* direction, avg	Modulus, psi
10.12	CN	−0.12	−0.10	0.98	3.8×10^6
10.09	CN	−0.10	−0.09	1.07	3.4×10^6
10.15	SN	−0.16	−0.12	0.98	4.2×10^6
10.04	SN	−0.14	−0.13	1.01	4.1×10^6

responsible for the variations observed among flexure tests performed in various orientations under different loading conditions, both as a result of increased surface damage and shear stress loads. Continuously nucleated specimens on the other hand, having higher interlaminar strengths, were able to resist machine damage to a greater degree and were better able to bear the resolved shear stresses imposed during flexure tests in the parallel orientation. Consequently, this material shows less difference between three and four point loading results than does surface nucleated material. Differences between parallel and perpendicular loading are also smaller than they are for surface nucleated specimens.

V. Conclusions

The experimental values obtained for both surface and continuously nucleated pyrolytic graphite indicate that the material has a considerably higher and more reliable strength at room temperature (18,000 ± 2000 psi) than has been appreciated. It is felt that this is primarily due to careful specimen preparation particularly with respect to the machining of basal plane edges. The effect of improved production techniques cannot be evaluated separately, but they probably contribute to greater reliability and strength through the availability of thicker and flatter material having fewer large nodules.

The difference between surface and continuously nucleated pyrolytic graphite with respect to response to mechanical tests occurs chiefly through the greater degree of interlocking of cones among the planes in the latter. This is brought out most clearly in torsional test results, although the same effect is apparent in flexure test results in which premature failure by delamination was characteristic of surface nucleated material. Table 6 summarizes the data presented and illustrates these similarities and differences between surface nucleated and continuously nucleated pyrolytic graphite as they are currently manufactured.

Although these illustrate the effects of microstructure on the mechanical properties as determined in relatively straightforward tests, there are other factors that enter into the choice of a pyrolytic graphite for a particular use. For example, residual stresses and batch to batch variations may change the relative levels of strength achieved by material with a given structure. The geometry of complex shapes also enters the picture through such factors as residual stresses, thickness variations, and radius of curvature ratios. However, although it may not be possible to predict ultimate allowable stresses in such cases, observations made of structure effects in simple tests permit qualitative estimates to be made of the probable influence that these more obscure phenomena will have. This can be of great help in preliminary design work with pyrolytic graphite.

Considerably more detailed attention is also being given to fracture mechanisms of pyrolytic graphite and the part played by surface damage. A more extended report regarding these considerations has recently been presented.[9]

Table 6 Mechanical properties of current production pyrolytic graphite (average values)

Test	Temp., °F	CN		SN	
Tensile, psi	75	17,818		18,191	
	3000	18,488		16,919	
	4000	27,525		22,095	
	5000	55,275		50,525	
Torsion, psi	75	2,578		1,522	
	3000	2,652		1,374	
	4000	3,135		1,469	
	5000	3,248		1,620	
		Parallel	Perpendicular	Parallel	Perpendicular
Bend 3 pt, psi	75	20,030	23,880	16,000	20,570
	3000	23,530	27,800	17,300	21,200
	4000	32,230	31,000	20,530	23,500
	5000	(no failure)	(no failure)	23,000	29,100
Bend 4 pt, psi	75	19,110	22,960	12,140	17,470
	3000	22,270	25,900	12,370	19,670
	4000	28,200	31,033	14,670	16,370
	5000	(no failure to 29,700)	(no failure to 26,600)	...	(no failure to 46,400)
Elastic modulus, 10^6 psi	75	3.5		4.5	
	3000	3.4		3.5	
	4000	2.7		3.0	
	5000	1.4		2.3	
Poisson's ratio, 75°F	Substrate side top	−0.095		−0.13	
	surface *c* direction	−0.11		−0.15	
		1.02		0.99	
Coeff. of Expansion, in./in./°F:					
a 2500–4500°F		2.1×10^{-6}		2.0×10^{-6}	
c RT − 4500°F		14.2×10^{-6}		15.0×10^{-6}	

References

[1] Pappis, J., "The mechanical properties of pyrolytic graphite," *Mechanical Properties of Engineering Ceramics*, edited by W. Kriegel and H. Palmour III (Interscience Publishers, Inc., New York, 1960), Chap. 25, pp. 429–450.

[2] Lozier, W. W. and Manofsky, M. B., "Properties and performance of pyrolytic graphite," *Mechanical Properties of Engineering Ceramics*, edited by W. Kriegel and H. Palmour III (Interscience Publishers, Inc., New York, 1960), Chap. 26, pp. 351–473.

[3] Diefendorf, R. J. and Stover, E. R., "Pyrolytic graphite—how structure affects properties," Metals Progr. **81**, 103–108 (1962).

[4] Schiff, D., "Pyrolytic materials for re-entry applications," Metals Engineering Quarterly **2**, 32–42 (1962).

[5] Riley, M. W., "The new world of graphite," Mater. Design Eng. **56**, 113–128 (1962).

[6] Pappis, J. and Blum, S., "Properties of pyrolytic graphite," J. Am. Ceram. Soc. **44**, 592–597 (1961).

[7] "Pyrolytic graphite data book," Lockheed Missile and Space Div. LMSD 288186 (April 14, 1961).

[8] Smith, W. H., "Mechanical properties of pyrolytic graphite—2. Effect of structure on strength at room temperature," General Electric Co. Memo. MF109, Part F (May 1960).

[9] Berry, J. M. and Gebhardt, J. J., "Interpretation of room temperature mechanical properties tests on pyrolytic graphite," J. Am. Ceram. Soc. (to be published).

[10] *The Industrial Graphite Engineering Handbook*, (Carbon Products Division, Union Carbide Corp., New York, Revised April 1964).

[11] Stover, E. R., "Flame polishing pyrolytic graphite," Metals Progr. **83**, 112–113 (1963).

FEBRUARY 1965 AIAA JOURNAL VOL. 3, NO. 2

Influence of Cushion Stiffness on the Stability of Cushion-Loaded Cylindrical Shells

D. O. BRUSH*
University of California, Davis, Calif.

AND

E. V. PITTNER†
Lockheed Missiles and Space Company, Palo Alto, Calif.

This paper presents results of a theoretical analysis of the influence of cushion stiffness on the buckling strength of cylindrical shells subjected to soft elastic cushion pressure. A stability equation is derived for a simply supported cylinder subjected to an axisymmetric band of cushion pressure applied at an arbitrary distance from one end of the cylinder. An exact solution is given for the limiting case of a circular ring or infinitely long cylinder under uniform elastic cushion pressure. For the more general case of a finite-length cylinder with an arbitrarily located band of cushions, infinite series are utilized in the solution. Extensive numerical results are presented in graphical form. They indicate that buckling pressures in general are much higher under cushion loading than under fluid-pressure loading. They also indicate that cylinder length and cushion location are unimportant unless the cylinder is rather short or the cushion is near one end. In such cases, however, the stabilizing influence of end rings is quite strong. Results are in agreement with previously available theoretical results for various limiting cases and with limited available test data.

Nomenclature

D	=	bending stiffness
E	=	Young's modulus
J_3	=	Eq. (8)
$K_m{}^n$	=	Eq. (9)
K_s	=	cushion stiffness coefficient, Eq. (A4)
L	=	length of cylindrical shell
V	=	total potential energy
W_s	=	work of cushion pressure
a	=	middle-surface radius
b	=	cushion width
c	=	distance from center of cushion to near end of cylinder
h	=	shell thickness
h_s	=	cushion thickness at impending buckling
k, m, n	=	wavelength parameters, Eq. (3)
p	=	pressure applied to cylinder by cushion
p_{cr}	=	buckling pressure
q	=	number of circumferential waves in buckled form
v, w	=	nondimensional tangential and radial displacement components of a point on the shell's middle surface; the corresponding distances are av, aw, and w is positive inward
α	=	L/a
ν	=	Poisson's ratio
η_m, ψ_k, J_1	=	Eq. (3)
λ	=	cushion thickness parameter, Eq. (A4)

Subscripts

0	=	prebuckling quantities
1	=	incremental quantities
s	=	cushion

Received May 1, 1964; revision received August 28, 1964.

* Professor of Engineering; formerly Senior Staff Scientist, Research Laboratories, Lockheed Missiles and Space Company, Palo Alto, Calif. Member AIAA.

† Research Specialist, Research Laboratories. Member AIAA.

Introduction

RADIAL pressure applied to the lateral surface of a rocket motor case by soft elastic cushions induces compressive hoop stresses in the motor case skin. If the cushions are suf-